RESEARCH ARTICLE

CLIMATE

Aerosol-cloud-climate cooling overestimated by ship-track data

Franziska Glassmeier[1,2,3]*, Fabian Hoffmann[3,4,5], Jill S. Johnson[6], Takanobu Yamaguchi[3,4], Ken S. Carslaw[6], Graham Feingold[4]

The effect of anthropogenic aerosol on the reflectivity of stratocumulus cloud decks through changes in cloud amount is a major uncertainty in climate projections. In frequently occurring nonprecipitating stratocumulus, cloud amount can decrease through aerosol-enhanced cloud-top mixing. The climatological relevance of this effect is debated because ship exhaust only marginally reduces stratocumulus amount. By comparing detailed numerical simulations with satellite analyses, we show that ship-track studies cannot be generalized to estimate the climatological forcing of anthropogenic aerosol. The ship track–derived sensitivity of the radiative effect of nonprecipitating stratocumulus to aerosol overestimates their cooling effect by up to 200%. The offsetting warming effect of decreasing stratocumulus amount needs to be taken into account if we are to constrain the cloud-mediated radiative forcing of anthropogenic aerosol.

Clouds interact with atmospheric radiation and therefore play an important role in the planetary energy balance. Their net effect is to cool the planet by reflecting incoming solar radiation (*1*). Covering large parts of the subtropical oceans, stratocumulus (Sc) clouds are by far the largest contributor to this cooling (*2*). Effects on cloud reflectivity caused by the production of atmospheric aerosol particles are the most uncertain anthropogenic forcing of the climate system (*3*, *4*). As an illustration of this effect, exhaust from ships can create "ship tracks" that manifest as bright linear features in Sc decks. This brightening arises because exhaust-aerosol particles act as nuclei of cloud droplets. A greater abundance of particles means that a cloud consists of more, but smaller, droplets, which enhances the radiant energy reflected to space (*5*). Changes in the number and size of cloud droplets also influence cloud physical processes (*6*–*11*); for the example of ship tracks, this means that the amount of cloud water inside and outside of a track may evolve differently. Globally, the large uncertainty in the cloud-mediated aerosol forcing arises from the unknown magnitude of such adjustments of cloud water in response to aerosol-induced perturbations (*3*, *12*, *13*). Here, we show that despite providing a illustration of aerosol-cloud interactions, ship tracks do not provide suitable data to estimate the magnitude of cloud liquid-water adjustments in a polluted climate, in contrast with the common assumption that ship-track data can quantify those adjustments (*14*–*17*).

In nonprecipitating Sc with their approximately full cloud cover, cloud response to aerosol perturbations is commonly quantified by the sensitivity (*4*, *18*, *19*)

$$S = \frac{\mathrm{d}A_\mathrm{c}}{\mathrm{d}N} = \frac{A_\mathrm{c}(1-A_\mathrm{c})}{3N}\left(1+\frac{5}{2}\frac{\mathrm{dlnLWP}}{\mathrm{dln}N}\right) \quad (1)$$

of cloud albedo A_c to cloud droplet number N. The first term on the right-hand side of Eq. 1 quantifies the albedo effect of changing droplet number when keeping the vertically integrated amount of liquid water, or liquid-water path (LWP), constant; the second term accounts for cloud water adjustments as quantified by the relative sensitivity $\mathrm{dlnLWP}/\mathrm{dln}N$ of LWP to N. Numerical values for LWP adjustments $\mathrm{dlnLWP}/\mathrm{dln}N$ have been derived from detailed modeling and satellite studies (*8*, *14*–*17*, *20*–*25*). Both approaches have recently converged on the insight that the sign of LWP adjustments is regime-dependent (Fig. 1). Adjustments tend to be positive under precipitating conditions where the addition of particles decreases drop size, increases colloidal stability, and allows for an accumulation of liquid water (*6*). A positive LWP adjustment thus implies thicker, more reflective clouds that have a stronger cooling effect. In the current work, we focus on nonprecipitating Sc. Morphologically, this regime features an approximately hexagonal arrangement of cloudy (closed) cells, whereas the precipitation-dominated regime tends to occur as an inverse pattern of open cells (*14*, *26*). Occurring in 50 to 80% of observations, the nonprecipitating regime is at least as common as the precipitating regime (*25*, *27*). Nonprecipitating Sc feature negative adjustments, indicating a decrease in LWP for higher aerosol concentrations. The decrease in LWP stems from the accelerated and stronger evaporation of cloud liquid in higher aerosol conditions as the Sc mixes with dry air from above the cloud (entrainment). Smaller droplets evaporate more efficiently because they provide a larger surface (for a given total amount of liquid) and reside closer to the entrainment interface than larger droplets owing to reduced gravitational settling, which increases the potential for evaporation (*7*–*11*, *28*). Negative LWP adjustment values indicate thinner, less reflective clouds and a weaker cooling effect. When the darkening effect of cloud thinning is stronger than the brightening of increased N, negative LWP adjustments can even imply a warming effect. In nonprecipitating Sc, this is the case when $\mathrm{dlnLWP}/\mathrm{dln}N < -2/5$ such that Eq. 1 becomes negative (orange shading in Fig. 1).

In addition to the distinction between the entrainment- and precipitation-dominated regimes, satellite studies have identified above-cloud moisture as an important control on the magnitude of LWP adjustments in Sc (*15*, *25*, *29*). This is consistent with process understanding from detailed cloud modeling studies [large-eddy simulation (LES)], where drier above-cloud conditions correspond to a stronger aerosol effect on entrainment (Fig. 1). As another factor behind the variability of adjustment estimates, the effects of N-LWP covariability that results from large-scale covariability of aerosol and moisture are discussed in (*15*, *30*). As an example of this confounding effect, compare a maritime situation with a clean and moist atmosphere to a polluted and drier continental case. Observations from these two cases will likely show that higher N is correlated with lower LWP, suggesting a negative LWP adjustment. Clearly, the "adjustment" quantified here is not related to the effect of aerosol on cloud properties driven by entrainment or precipitation formation that we seek to capture but rather to large-scale conditions.

A special appeal of ship tracks has been that they are not affected by external covariability because the large-scale meteorological conditions are the same inside and outside of the track. Accordingly, results from targeted satellite analyses of ship tracks (*14*, *16*, *20*) have been assigned higher credibility than climatological satellite studies, for which external covariability cannot be ruled out. In particular, the comparably large absolute adjustment values found in the latter studies have been attributed to aerosol-moisture covariability, assuming that weak-to-almost absent LWP adjustments identified by ship-track studies

[1]Department of Geoscience and Remote Sensing, Delft University of Technology, P.O. Box 5048, 2600 GA Delft, Netherlands. [2]Department of Environmental Sciences, Wageningen University, P.O. Box 47, 6700 AA Wageningen, Netherlands. [3]Cooperative Institute for Research in Environmental Sciences, University of Colorado Boulder, Boulder, CO 80309, USA. [4]NOAA Chemical Sciences Laboratory, 325 Broadway, Boulder, CO 80305, USA. [5]Institut für Meteorologie, Ludwig-Maximilians-Universität, Theresienstrasse 37, 80333 München, Germany. [6]School of Earth and Environment, University of Leeds, Woodhouse Lane, Leeds LS2 9JT, UK.
*Corresponding author. Email: f.glassmeier@tudelft.nl

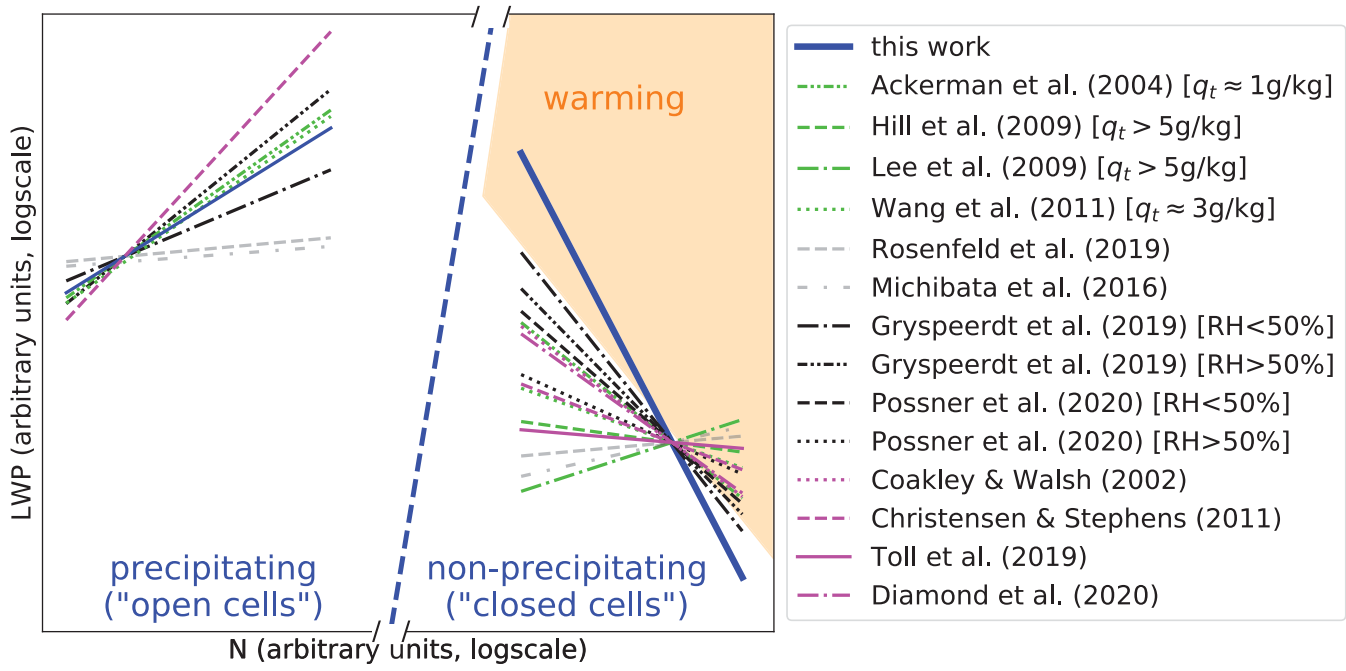

Fig. 1. Reported log-log-linear relationships between LWP and *N* in comparison to this work. Lines are based on reported slopes (table S1), and axis intercepts have been added as suitable for illustration. The dashed blue line indicates a critical droplet radius for precipitation formation (based on a mean droplet radius of 12 μm at cloud top for an adiabatic condensation rate of 2.5 × 10^{-6} kg m^{-4}), which separates the precipitation-dominated regime on the left from the nonprecipitating, entrainment-dominated regime on the right. The latter is the focus of this study. Colors distinguish results from LESs (green), climatological satellite studies (black), and satellite studies of ship tracks (magenta). Results in gray are shown for completeness but are not directly comparable, owing to differences in methodology. For simulation and climatological studies, above-cloud absolute humidity (q_t) or ranges of relative humidity (RH) are indicated. Solid blue lines show values derived in this work (tables S1 and S4; in particular, dlnLWP/dln*N* = −0.64 in the entrainment regime). The orange shading indicates where LWP adjustments are sufficiently negative to lead to climate warming rather than cooling based on the sign of albedo sensitivity *S* (Eq. 1).

(*14*, *16*, *20*) provide the best estimate for LWP adjustment. In contrast to this assumption, a recent study of a shipping lane reports considerably negative adjustment values (*17*).

We show that the current emphasis on satellite studies of ship tracks to estimate LWP adjustments leads to an overestimation of the cooling effect of aerosols in Sc. We furthermore reconcile the broad range of reported adjustment estimates and discuss implications of our results for identifying alternatives to ship-track studies. Our argument is illustrated in Fig. 2 and builds on two key results: (i) LWP adjustments become more negative as Sc decks evolve toward a steady state, and (ii) in ship tracks, this temporal evolution does not proceed long enough to be representative of Sc decks in a polluted climate.

Effect of cloud field evolution toward steady state on adjustment strength

Climatological satellite studies derive LWP adjustments dlnLWP/dln*N* as slopes of linear regression lines through median LWP values in *N*-bins. We apply this methodology to an ensemble of 12-hour-long LES time series that resembles the scope of a satellite dataset (supplementary materials). To discuss the time dependence of adjustments, we separately derive LWP adjustments per time step. Figure 3A and fig. S1A illustrate this for t = 2 hours (magenta) and t = 12 hours (green). Considering all time steps 2 hours ≤ t ≤ 12 hours shows that the LWP adjustment becomes increasingly negative over time (Fig. 3B). This behavior results from the sampling of the *N*-LWP space by our simulations, which evolves over time. By construction, our dataset initially features an uncorrelated sampling (supplementary materials). This explains the almost horizontal regression line and corresponding vanishing adjustment observed at t = 2 hours. An initial covariability of *N* and LWP values would have imprinted an initial correlation and corresponding adjustment value between *N* and LWP.

As our simulations collectively evolve further from the initial state, they approach a steady-state LWP line (blue curve in Fig. 3A and fig. S1) and the sampling of the *N*-LWP space features an increasingly negative correlation. This relationship replaces the initial relationship because the evolution speed of Sc systems scales with their distance to the steady-state line (fig. S3). Had we run our simulations beyond 12 hours, all ensemble members would eventually have reached their steady-state LWP. This means that for $t \to \infty$ only the steady-state line is sampled and the LWP adjustment is quantified by the slope of this line. Because the slope of the steady-state LWP line reflects the *N*-dependence of entrainment (*31*), the LWP adjustment at $t \to \infty$, $d\ln LWP_\infty/d\ln N$, is a direct quantification of *N*—or more generally aerosol—effects on cloud processes.

Using Gaussian-process emulation, we determine the location of this steady-state line in *N*-LWP space from limited-duration time series (supplementary materials). For nonprecipitating Sc, we obtain $d\ln LWP_\infty/d\ln N = -0.64$ (Fig. 3A; uncertainty quantification in table S4). This value constitutes a lower bound; a more negative adjustment value would require a stronger *N*-dependent entrainment and therefore drier above-cloud conditions than prescribed for our simulations. This is not realistic because our simulations feature very dry conditions already (fig. S5 and table S2). Figure 1 also supports −0.64 ≤ dlnLWP/dln*N* as a lower bound on previous estimates from the literature. We contrast this value with the positive value of the precipitation-dominated branch, for which we determine a slope of 0.21 (table S4) that lies well within the reported range (Fig. 1).

The equilibration of adjustments to the steady-state value is the collective result of the equilibration of individual Sc systems.

This allows us to derive that the observed time dependence of LWP adjustments is well described as an exponential decay toward $d\ln LWP_\infty/d\ln N$ (Fig. 3B)

$$\mathrm{adj}(\Delta t) = \frac{d\ln LWP_\infty}{d\ln N}\left[1 - \exp\left(-\frac{\Delta t}{\tau_{adj}}\right)\right],$$

$$\tau_{adj} \approx \tau\left(1 - 1.6\,\frac{d\ln LWP_\infty}{d\ln N}\right) = 2.0\,\tau = 20 \text{ hours} \quad (2)$$

with an adjustment equilibration time scale τ_{adj} that scales with the equilibration time scale of an individual system, τ = 9.6 hours, and with adjustment strength (supplementary materials). The time dependence of LWP adjustments on a time scale of almost a day is in marked contrast to the radiative effect of an increased cloud droplet number, which takes full effect in 5 to 10 min (supplementary materials).

The extent and interpretation of LWP adjustments in a Sc field depends on the proximity of the system's LWP to its steady-state LWP. Adjustments based on sampling transient LWP, far from steady state, reflect *N*-LWP covariability that is externally prescribed on the system, i.e., a mere association; LWP adjustments diagnosed from steady systems reflect aerosol-dependent cloud processes, i.e., a causal relationship; intermediate degrees of proximity result in a mixture of both.

Insufficient time for evolution of ship tracks toward steady state

The degree of proximity of an ensemble, or sampling, of Sc systems to its steady-state LWP adjustment can be estimated by comparing the duration of its evolution under an aerosol perturbation, Δt, to the characteristic adjustment equilibration time scale, τ_{adj} = 20 hours (Eq. 2). From a Lagrangian perspective, a Sc system is exposed to an aerosol background throughout its lifetime: In the absence of precipitation, the aerosol coevolves with the boundary layer height (*25*), i.e., on a multiday-long time scale (*32*). Typical Sc trajectories in the subtropics persist on time scales of days, Δt_{clim} > 48 hours, before they transition into the shallow cumulus regime owing to advection toward higher sea-surface temperatures (*33*). Because $\Delta t_{clim} \gg \tau_{adj}$, the climatological sampling of Sc is dominated by strongly equilibrated LWPs. Although not necessarily composed of steady-state LWPs, we can assume that the LWP climatology of non-precipitating Sc is better characterized as a sampling of steady-state LWPs than as one of highly transient LWPs. Steady-state values as a feasible approximation for Sc properties are in line with previous theoretical studies (*34*). A substantial probability of Sc being observed close to their steady state is also consistent with relatively narrow climatological distributions of Sc LWPs (*15*, *35*) that indicate dominant sampling of a steady-state line. The scatter around this line corresponds to transient LWPs.

Sc decks being strongly adjusted to the aerosol background in which they evolve has implications for constraining the anthropogenic radiative forcing; LWP adjustments need to compare Sc that are strongly adjusted to an aerosol background typical of an industrial-era aerosol climatology (cyan circle in Fig. 4) to Sc decks that are strongly adjusted to a pre-industrial aerosol background (orange circle). Climatological satellite studies are suitable for this quantification because they predominantly sample strongly adjusted LWPs close to steady state. As discussed in the previous section, this specifically means that such studies capture cloud processes and are only weakly confounded by externally induced *N*-LWP covariability.

Ship-track data are obtained throughout the life of the track, with fresh tracks more likely to be sampled owing to their better visibility. With a typical lifetime for ship tracks of 6 to 7 hours (*36*, *37*), this corresponds to an average evolution time until sampling of $\Delta t_{ship} \approx 3$ hours. Because the characteristic equilibration time exceeds the typical evolution time at sampling, $\Delta t_{ship} \ll \tau_{adj}$, we conclude that LWPs sampled from ship tracks are not representative of the aerosol-cloud interaction processes, specifically entrainment, that manifest as a Sc system approaches a steady-state LWP. Instead, their sampling of transient LWPs carries a strong imprint of their specific initial conditions. To characterize these conditions, we describe ship-track studies as a sampling within two different *N*-bins, one representing out-of-track conditions and the other in-track conditions (Fig. 4). Because LWP adjustments are not instantaneous, the LWP distributions within these two bins are identical when the ship exhaust first makes contact with the cloud. As for the idealized initial conditions in our dataset, this corresponds to an initial adjustment of zero (purple regression line in Fig. 4). After the perturbation, the in-track distribution evolves toward an asymptotic LWP value that is different from that of the out-of-track LWP. Owing to the short duration of this evolution until sampling, adjustment values diagnosed from ship tracks remain small. Indeed, evolution according to Eq. 2 corresponds to an adjustment value of

$$\mathrm{adj}(\Delta t_{ship} = 3 \text{ hours}) = -0.1$$

which matches reported values ranging from −0.2 to 0.0 (table S1). By contrast, when sampling a climatologically polluted situation, adjustments can evolve toward more

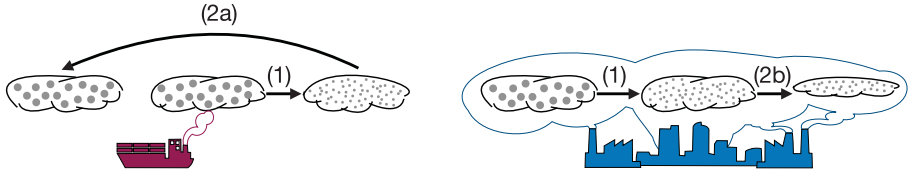

Fig. 2. LWP adjustments in ship tracks as compared with industrial-era pollution. As an initial response to the aerosol perturbation, both situations feature cloud brightening through more, but smaller, cloud droplets at constant LWP (step 1). The ship track then returns to its original state because the perturbation ceases after a few hours (step 2a). An aerosol background that is enhanced because the climatological aerosol background is perturbed, by contrast, persists for days and allows for LWP to equilibrate toward a new steady state that is characterized by increased entrainment efficiency and a lower LWP (step 2b).

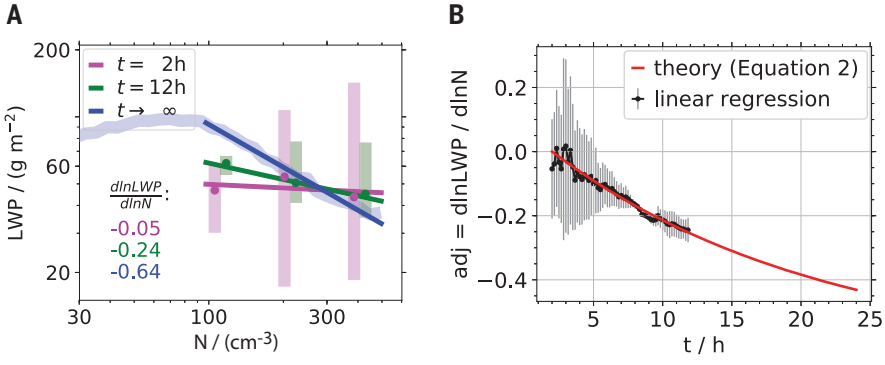

Fig. 3. Time dependence of LWP adjustments. (**A**) Data points with error bars show median and 25th-75th percentile of simulated LWP at t = 2 hours (magenta) and t = 12 hours (green) for the *N*-bins indicated in fig. S1A. The light blue curve indicates the steady-state LWP as in Fig. S1. Regression lines with slopes $d\ln LWP/d\ln N$ are indicated. (**B**) Each data point indicates an adjustment slope obtained as in (A), with error bars for 2 hours ≤ t ≤ 12 hours. The red line shows the theoretically expected exponential decay (Eq. 2).

negative values before being sampled and values of adj(Δt_{clim} = 48 hours) = −0.6, close to the asymptotic value of −0.64 (Fig. 3A), are obtained.

Although ship exhaust may, at first glance, seem to be an intriguing proxy for aerosol conditions typical of the industrial-era aerosol climatology, it does not perturb the pristine background for a sufficiently long time (Fig. 2). In other words, typical LWPs in ship tracks are not comparable to LWPs in Sc that experience a higher aerosol background owing to an anthropogenic shift of the aerosol climatology (cyan circle versus triangle in Fig. 4).

Implications for the cloud-mediated radiative forcing of anthropogenic aerosol

Ship track–derived LWP adjustments are less negative than the LWP adjustment exhibited by a Sc deck under climatologically polluted conditions. Because negative adjustments mean that an increased aerosol load leads to cloud thinning and reduced reflectivity, they imply a warming effect that offsets the cooling associated with cloud brightening (Eq. 1). Ship-track studies underestimate this offsetting warming effect of LWP adjustments (Fig. 2). We contend, therefore, that using ship track–derived adjustment values to estimate the cloud-mediated radiative forcing of anthropogenic aerosol underestimates the absolute effect of LWP adjustments on the radiative forcing. With $-0.64 \leq d\ln LWP/d\ln N$ as a lower bound (Fig. 3), this underestimation corresponds to an overestimation of the cooling effect of aerosols on nonprecipitating Sc of up to 200% (supplementary materials). Because nonprecipitating Sc occur frequently (*25*, *27*), this warming effect may offset the cooling effect of positive LWP adjustments in precipitating Sc in the overall climate effect of Sc.

Our results are consistent with recent satellite estimates of LWP adjustments in Sc (*15*, *25*). Our insight that the effects of external covariability fade as a Sc system evolves toward its internal steady state refutes *N*-LWP covariability as the likely explanation for the strongly negative adjustment values reported. At the same time, our modeling results show that strongly negative adjustment values are consistent with process understanding. In combination with the limitations of ship track–derived adjustment values discussed above, we therefore conclude that climatological satellite studies should be assigned more weight for estimating LWP adjustments than ship-track studies. Specifically, values of $d\ln LWP/d\ln N$ = −0.3 (*25*) to −0.4 (*15*) should be considered possible central values rather than lower bounds, as in a recent review (*4*). Our analysis establishes the steady-state adjustment $d\ln LWP_\infty/d\ln N$ = −0.64 as a new lower bound for LWP adjustments in nonprecipitating Sc.

Our results are moreover consistent with a recent study that derived LWP adjustments from climatological observations of a heavily frequented shipping lane (*17*). This setup provides more persistent pollution than an individual ship track while still suffering from a certain intermittency of pollution as compared with a climatological perturbation. We estimate an effective lifetime of ship tracks in a shipping lane of $\Delta t_{lane} \gtrsim 9$ hours (supplementary materials). With an evolution time that is longer than that for individual ship tracks but shorter than Sc lifetime, it is not surprising that the shipping lane provides a numerical adjustment value that lies in between those derived from single-ship-track studies and fully climatological studies (Fig. 1). Our results therefore reconcile and explain the differing LWP adjustments that have recently been reported (*15*–*17*, *25*).

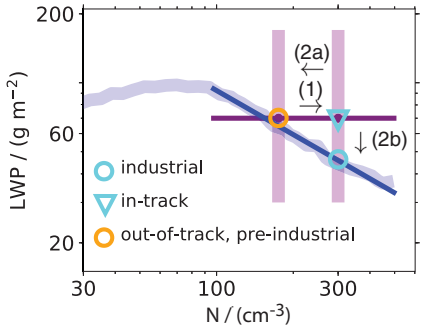

Fig. 4. Conceptual illustration of LWP adjustments as derived from ship tracks in comparison to climatological satellite studies. (Pre)industrial climatological conditions are strongly adjusted and represented by circles close to the steady state (blue). LWPs within ship tracks are weakly adjusted (triangle) such that ship-track studies are based on comparing almost identical LWP distributions (purple dots with error bars; illustration in analogy to Fig. 3A, no actual data), which implies vanishing LWP adjustments (purple regression line). Labeled arrows correspond to steps shown in Fig. 2.

Satellite remote sensing of thin and broken clouds remains a challenge, with large uncertainties in retrieved values. Despite the support for climatological satellite studies that our results provide, it therefore seems desirable to identify alternatives to ship-track studies that allow for a direct observation of aerosol effects. Our analysis shows that suitable natural experiments should feature temporally continuous pollution. Spatial continuity of pollution is another criterion, which excludes biases from boundary effects as described for ship tracks (*38*, *39*). Effusive volcanic emission and oceanic outflows of continental air are examples of such continuously polluting natural experiments. Existing datasets do not sample the subtropical Sc regions, however (*16*). In addition to adjustments being cloud-regime specific, higher extratropical above-cloud moisture may bias toward less-negative values. Undersampling of the subtropics may also exacerbate the time-scale effect, leading to underestimation of negative anthropogenic LWP adjustments by ship-track data.

Deliberate experiments could, by design, provide suitable aerosol perturbations. Such experiments have been suggested to assess the feasibility of marine cloud brightening (MCB) (*40*), i.e., the advertent mitigation of climate forcing by injecting aerosol into extensive Sc decks. In contrast to a setup with persistent pollution as needed to estimate the climatological aerosol effect, MCB rests on the notion of weak LWP adjustments as observed in ship tracks. Our results indicate that an intermittent aerosol perturbation may maximize the cooling effect by limiting the magnitude of compensating adjustments. To be feasible, MCB strategies will therefore have to balance the potential for LWP adjustments discussed here with the total aerosol perturbation obtainable with a given installation.

There is an urgent need to quantify the albedo and LWP responses in both precipitating and nonprecipitating Sc cloud systems to successfully quantify the cloud-mediated effect of anthropogenic aerosol on the climate system. This will require careful assessment of the frequency of occurrence and areal coverage of these regimes, with attendant consideration of the temporal nature of the LWP responses. Estimates of aerosol-cloud forcing that ignore the nonprecipitating regime are likely to substantially overestimate climate cooling.

REFERENCES AND NOTES

1. G. L. Stephens *et al.*, *Nat. Geosci.* **5**, 691–696 (2012).
2. T. S. L'Ecuyer, Y. Hang, A. V. Matus, Z. Wang, *J. Clim.* **32**, 6197–6217 (2019).
3. O. Boucher *et al.*, *Climate Change 2013: The Physical Science Basis. Working Group I Contribution to the Fifth Assessment Report of the Intergovernmental Panel on Climate Change*, T. F. Stocker *et al.*, Eds. (Intergovernmental Panel on Climate Change, 2013).
4. N. Bellouin *et al.*, *Rev. Geophys.* **58**, RG000660 (2020).
5. S. Twomey, *Atmos. Environ.* **8**, 1251–1256 (1974).
6. B. A. Albrecht, *Science* **245**, 1227–1230 (1989).
7. S. Wang, Q. Wang, G. Feingold, *J. Atmos. Sci.* **60**, 262–278 (2003).
8. A. S. Ackerman, M. P. Kirkpatrick, D. E. Stevens, O. B. Toon, *Nature* **432**, 1014–1017 (2004).
9. C. S. Bretherton, P. N. Blossey, J. Uchida, *Geophys. Res. Lett.* **34**, L03813 (2007).
10. J. D. Small, P. Y. Chuang, G. Feingold, H. Jiang, *Geophys. Res. Lett.* **36**, L16806 (2009).
11. F. Hoffmann, G. Feingold, *J. Atmos. Sci.* **76**, 1955–1973 (2019).
12. B. Stevens, G. Feingold, *Nature* **461**, 607–613 (2009).
13. J. Mülmenstädt, G. Feingold, *Curr. Clim. Change Rep.* **4**, 23–40 (2018).
14. M. W. Christensen, G. L. Stephens, *J. Geophys. Res.* **116**, D03201 (2011).
15. E. Gryspeerdt *et al.*, *Atmos. Chem. Phys.* **19**, 5331–5347 (2019).
16. V. Toll, M. Christensen, J. Quaas, N. Bellouin, *Nature* **572**, 51–55 (2019).
17. M. S. Diamond, H. M. Director, R. Eastman, A. Possner, R. Wood, *AGU Advances* **1**, e2019AV000111 (2020).
18. S. Platnick, S. Twomey, *J. Appl. Meteorol.* **33**, 334–347 (1994).
19. R. Boers, R. M. Mitchell, *Tellus A* **46**, 229–241 (1994).
20. J. A. Coakley Jr., C. D. Walsh, *J. Atmos. Sci.* **59**, 668–680 (2002).

21. A. A. Hill, G. Feingold, H. Jiang, *J. Atmos. Sci.* **66**, 1450–1464 (2009).
22. S. S. Lee, J. E. Penner, S. M. Saleeby, *J. Geophys. Res.* **114**, D07204 (2009).
23. H. Wang, P. J. Rasch, G. Feingold, *Atmos. Chem. Phys.* **11**, 4237–4249 (2011).
24. D. Rosenfeld *et al*., *Science* **363**, eaav0566 (2019).
25. A. Possner, R. Eastman, F. Bender, F. Glassmeier, *Atmos. Chem. Phys.* **20**, 3609–3621 (2020).
26. F. Glassmeier, G. Feingold, *Proc. Natl. Acad. Sci. U.S.A.* **114**, 10578–10583 (2017).
27. D. C. Leon, Z. Wang, D. Liu, *J. Geophys. Res.* **113**, D00A14 (2008).
28. H. Xue, G. Feingold, B. Stevens, *J. Atmos. Sci.* **65**, 392–406 (2008).
29. Y.-C. Chen, M. W. Christensen, G. L. Stephens, J. H. Seinfeld, *Nat. Geosci.* **7**, 643–646 (2014).
30. F. A.-M. Bender, L. Frey, D. T. McCoy, D. P. Grosvenor, J. K. Mohrmann, *Clim. Dyn.* **52**, 4371–4392 (2019).
31. F. Hoffmann, F. Glassmeier, T. Yamaguchi, G. Feingold, *J. Atmos. Sci.* **77**, 2203–2215 (2020).
32. W. H. Schubert, J. S. Wakefield, E. J. Steiner, S. K. Cox, *J. Atmos. Sci.* **36**, 1308–1324 (1979).
33. I. Sandu, B. Stevens, *J. Atmos. Sci.* **68**, 1865–1881 (2011).
34. C. S. Bretherton, J. Uchida, T. N. Blossey, *J. Adv. Model. Earth Syst.* **2**, 20 (2010).
35. R. Wood, *Mon. Weather Rev.* **140**, 2373–2423 (2012).
36. M. W. Christensen, K. Suzuki, B. Zambri, G. L. Stephens, *Geophys. Res. Lett.* **41**, 6970–6977 (2014).
37. P. A. Durkee *et al*., *J. Atmos. Sci.* **57**, 2542–2553 (2000).
38. H. Wang, G. Feingold, *J. Atmos. Sci.* **66**, 3257–3275 (2009).
39. Y.-C. Chen, M. W. Christensen, D. J. Diner, M. J. Garay, *J. Geophys. Res. Atmos.* **120**, 2819–2833 (2014).
40. R. Wood, T. Ackerman, P. Rasch, K. Wanser, *Earths Futur.* **5**, 659–663 (2017).

ACKNOWLEDGMENTS

F.G. thanks A. Possner and T. Goren for helpful discussions about the interpretation of satellite literature. M. Khairoutdinov graciously provided the System for Atmospheric Modeling (SAM) model. The University of Wyoming, Department of Atmospheric Science, is acknowledged for archiving the radiosonde data. We thank three anonymous reviewers for their helpful comments. **Funding:** F.G. acknowledges support from The Branco Weiss Fellowship – Society in Science, administered by the ETH Zürich, and from a Veni grant of the Dutch Research Council (NWO). F.H. held a visiting fellowship of the Cooperative Institute for Research in Environmental Sciences (CIRES) at the University of Colorado Boulder, and the NOAA Earth System Research Laboratory, and is supported by the German Research Foundation under grant HO 6588/1-1. J.S.J. and K.S.C. were supported by the Natural Environment Research Council (NERC) under grant NE/I020059/1 (ACID-PRUF) and the UK-China Research and Innovation Partnership Fund through the Met Office Climate Science for Service Partnership (CSSP) China as part of the Newton Fund. K.S.C. is currently a Royal Society Wolfson Research Merit Award holder. This research was partially supported by the Office of Biological and Environmental Research of the U.S. Department of Energy Atmospheric System Research Program Interagency Agreement DE-SC0016275 and by an Earth's Radiation Budget grant, NOAA CPO Climate & CI #03-01-07-001. **Author contributions:** F.G., G.F., and F.H. conceived the study; F.G. developed the emulator with support from J.S.J. and K.S.C.; T.Y. performed the simulations. All authors contributed to the final product. **Competing interests:** All authors declare that they have no competing interests. **Data and materials availability:** Simulation data are available from https://esrl.noaa.gov/csl/groups/csl9/datasets/data/cloud_phys/2020-Glassmeier-etal/. Radiosonde data can be acccessed at http://www.weather.uwyo.edu/upperair/sounding.html.

SUPPLEMENTARY MATERIALS

science.sciencemag.org/content/371/6528/485/suppl/DC1
Materials and Methods
Supplementary Text
Figs. S1 to S6
Tables S1 to S4
References (*41*–*45*)

23 June 2020; accepted 22 December 2020
10.1126/science.abd3980